MICROSOLVATION OF THE CN RADICAL AND ANION: COMPETITION BETWEEN HYDROGEN BONDING AND ELECTROSTATIC NON-COVALENT INTERACTIONS

by

JACOB W. G. BLOOM

(Under the Direction of H. F. Schaefer)

ABSTRACT

A theoretical study of microsolvated CN radical and anion with water has been carried out. CN anion has long held the interest of chemists as a pseudohalide. CN radical and water are of interest to both astrophysics and biochemistry. A theoretical study of the microsolvated system should prove useful in future studies. Furthermore, this work illustrates the competition between hydrogen bonding and electrostatic non-covalent interactions. This study benchmarks density functional theory results for the zero and one water cases of both the radical and anion against focal point analysis. Further benchmark of the vertical detachment energies of the anion systems to experiment is also shown. The density functional theory is carried out through the four water case. Hydration energies, frequencies, dipole moments, and vertical and adiabatic electron affinities were computed for both the radical and anion systems.

INDEX WORDS: Cyanide, Cyanyl, Microsolvation

MICROSOLVATION OF THE CN RADICAL AND ANION: COMPETITION BETWEEN HYDROGEN BONDING AND ELECTROSTATIC NON-COVALENT INTERACTIONS

by

JACOB W. G. Bloom

B.A., New College of Florida, 2009

A Thesis Submitted to the Graduate Faculty of The University of Georgia in Partial Fulfillment of the Requirements for the Degree

MASTER OF SCIENCE

ATHENS, GEORGIA

2010

MICROSOLVATION OF THE CN RADICAL AND ANION: COMPETITION BETWEEN HYDROGEN BONDING AND ELECTROSTATIC NON-COVALENT INTERACTIONS

by

JACOB W. G. BLOOM

Major Professor: H. F. Schaefer

Committee: G. Smith
N. Adams

Electronic Version Approved:

Maureen Grasso
Dean of the Graduate School
The University of Georgia
December 2010

ACKNOWLEDGEMENTS

This work was supported by NSF grant NSF-CHE0749868. Thanks to S. E. Wheeler and H. F. Schaefer for mentoring me throughout this process. Thanks to H. M. Jaeger for the fruitful discussions regarding electrostatic non-covalent interactions. Some figures were generated using HFSmol.[1]

TABLE OF CONTENTS

Page

LIST OF TABLES

Page

LIST OF FIGURES

Page

CHAPTER 1

INTRODUCTION

Non-covalent interactions (hydrogen bonding, π-π, electrostatic, *etc*.) have emerged as a fruitful area of research in recent decades, due in part to the pivotal role of such interactions in biological systems. $\cdot CN\cdots H_2O$ constitutes an intriguing system to study the competition between two prototypical non-covalent interactions: hydrogen bonding and dipole-quadrupole complexes. The nitrogen in ·CN is expected to function as a proton acceptor, while consideration of simple multipolar interactions suggests the formation of a complex between water and the carbon end of the CN radical.

Clusters of the CN radical (·CN) and water are of interest to both the fields of astrophysics and biochemistry. CN radical is found in cometary ices and in a variety of enzymes, though the precise chemistry of this simple diatomic radical has not been fully elucidated in either case. The origin of ·CN in comets is still unclear.[2] In biochemistry, the fate of CN radicals produced by the reaction of cyanide (CN^-) with horseradish peroxidase and mitochondrial cytochrome c oxidase is similarly unsettled.[3] A related issue is understanding the ability of the white rot fungus *Phanerochaete chrysosporium* to decompose environmental pollutants such as DDT, benzo[a]pyrene, and even cyanide.[4,5] This ability has the potential for environmental cleanup of areas contaminated by cyanide.[5]

Interest in CN radicals in cometary ice was spurred by work published in 1984 in which Bockelée-Morvan *et al.* showed that the upper limit of the rate of hydrogen cyanide production was lower than that of CN radical in comets.[6] Subsequently, many other possible parent

molecules for CN radical have been proposed, including cyanogens,[7] cyanoacetylene,[7,8] and diacetylene.[8] Another possible source of CN radical in comets is through direct accumulation from dust.[9] Dense interstellar clouds are composed of ices of water, carbon monoxide, carbon dioxide, methanol, hydrogen, methane, ammonia and cyanide-like species.[10] CN radical is of particular interest in this context since R-CN compounds constitute possible building blocks of amino acids.[11] Detailed studies of CN radical in a microsolvated environment will facilitate our understanding of the chemistry of cometary ice and interstellar clouds. Further study of ·CN and of the moon could help determine from where the water on the moon came, since one theory is that it accumulated from the very comets that contain CN.[12]

CN radical is involved in the study of proteins as well since cyanide is used as an inhibitor in the study of hemoproteins, including horseradish peroxidase and mitochondria cytochrome c oxidase.[13] Horseradish peroxidase converts cyanide to CN in the presence of hydrogen peroxide[14] and cytochrome c oxidase is able to convert without the presence of hydrogen peroxide[15]. In both cases, when cyanide is converted to ·CN, the enzymes are inhibited even further than if cyanide remains unchanged.[3] CN is thought to react with the iron protoporphyrin IX of horseradish peroxidase and a cysteine residue in cytochrome c oxidase.[3] The chemistry of CN radical in the presence of a small number of water molecules will be vital to understanding the fate of ·CN in these systems. These types of study can also benefit the environment through the white rot fungus. Lignin peroxidase H2 in white rot fungus behaves similarly to that of horseradish peroxidase, in that it can oxidize cyanide to CN when in the presence of hydrogen peroxide.[5] The CN is then further mineralized into carbon dioxide.[5]

Cyanide anion is present in both solutions and solids. It has many applications in coordination chemistry.[16] It is also very important in material science, yet there are limited

solvation studies of cyanide. Cyanide has been called a pseudohalide because it has many similar properties to halide anions, especially chlorine. Both have similar ionic radii, polarizabilities, electron binding energies, and hydration energies. They do differ, however, in that cyanide anions are not spherical like chloride anions and therefore prefers to complex on the ends.[16]

We report a theoretical study of the microsolvation of the CN radical in water, including detailed analyses of novel clusters of ·CN and water. As a comparison, and to study the evolution of the electron affinity of ·CN in a microsolvated environment, $CN^-(H_2O)_n$ clusters were also examined. $CN(H_2O)_n$ provides fertile ground for examining the competition between hydrogen bonding and electrostatic non-covalent complexes in a relatively simple system. Definitive relative energies of isomers of $\cdot CN\cdots H_2O$ and $CN^-\cdots H_2O$ were derived via systematic extrapolations of *ab initio* energies within the focal point approach (FPA) of Allen and co-workers.[17-20] Carefully calibrated density functional theory methods were used to study $\cdot CN(H_2O)_n$ and $CN^-(H_2O)_n$ (n = 0 – 3).

CHAPTER 2

THEORETICAL METHODS

This work uses both coupled cluster approximations and density functional theory. The coupled cluster is used in conjunction with focal point extrapolations with which the density functional theory is benchmarked. This section serves as an introduction to these computational methods.

Multipole Expansion

Multipole expansions can be a good way to estimate the interactions of molecules. If a molecule has only one strong multipole, then a further approximation can be made by ignoring the other multipoles.[21] Otherwise, the interaction of that molecule will be due to a mixture of multipoles. Multipole expansion is valid at distances significantly larger than the charge distributions that contribute to the multipoles.[21]

The multipole moments can be elucidated by starting with the definition of the scalar potential as:

$$\Phi(\vec{x}) = \int \frac{\rho(\vec{x}')}{|\vec{x} - \vec{x}'|} d^3x' .$$

This equation can be modified by replacing the absolute value part with a spherical harmonic expansion:

$$\Phi(\vec{x}) = 4\pi \sum_{l,m} \frac{1}{2l+1} \left[\int Y_{lm}^*(\theta', \phi') r'^l \, \rho(\vec{x}') d^3x' \right] \frac{Y_{lm}(\theta, \phi)}{r^{l+1}},$$

where $Y_{lm}(\theta, \phi)$ is a spherical harmonic.[21]

The scalar potential of a system at a point far from the charges in that system can also be described as:

$$\Phi(\vec{x}) = \sum_{l=0}^{\infty} \sum_{m=-l}^{l} \frac{4\pi}{2l+1} q_{lm} \frac{Y_{lm}(\theta,\phi)}{r^{l+1}}.$$

This is called the multipole expansion and the q_{lm} components are the multipole moments where l=0 is the monopole term, l=1 are the dipole terms, l=2 are the quadrupole terms.[21] By comparing these two equations, an expression for multipole moments can be found:

$$q_{lm} = \int Y_{lm}^{*}(\theta',\phi') r'^{l} \rho(\vec{x}') d^3x'.$$

Since the only m-dependent part in this multipole moment is in the spherical harmonic, q behaves in a similar fashion to that of the spherical harmonics for $-m$:

$$q_{l,-m} = (-1)^m q_{lm}^{*}.$$

These q multipole moments can be solved in terms of the total charge, dipole moments along the x, y, and z axes, quadrupole tensor terms, and higher order terms.[21]

To link the total charge, the three dipole moments, and the quadrupole tensor terms, the scalar potential can once again be expanded; this time, that same absolute term in the scalar potential is Taylor expanded:

$$\Phi(\vec{x}) = \int \rho(\vec{x}') d^3x' \frac{1}{r} + \int \rho(\vec{x}') \vec{x}' d^3x' \frac{\vec{x}}{r^3} + \frac{1}{2} \sum_{i,j} \int \rho(\vec{x}') \left[3x_i' x_j' - \delta_{ij} r'^2 \right] d^3x' \frac{x_i x_j}{r^5} + \cdots.$$

Plugging in for the dipole moments, this scalar potential becomes:

$$\Phi(\vec{x}) = \frac{q}{r} + \frac{\vec{p} \cdot \vec{x}}{r^3} + \frac{1}{2} \sum_{i,j} Q_{ij} \frac{x_i x_j}{r^5} + \cdots,$$

where q is the total charge, $\vec{p}$ are the dipole moments along the axes, and Q_{ij} are the quadruple tensor terms.[21]

Basic Quantum Theory

Good basis sets are extremely necessary in computational chemistry. Electrons are extremely well described by Slater-type orbitals. Unfortunately, analytical solutions to Slater-type orbitals in a reasonable amount of time are illusive.[22] A great breakthrough in computational studies came with the approximation of the Slater-type orbitals with Gaussian-type orbitals through integral transformations:[22]

$$e^{-\xi r} = \int_0^{\infty} \alpha^{\frac{-3}{2}} e^{-\xi^2/4\alpha} e^{-\alpha r^2} d\alpha.$$

This equation readily makes sense if a graph of a Slater function is compared to that of a linear combination of Gaussian functions fitted to that Slater function. Despite the increased number of integrals now required, since there are many Gaussian functions per Slater function, speed in computations has actually increased due to the ease with which a Gaussian function can be integrated.[22] Huzinaga makes note of the fact that the accuracy sacrificed in using a small set of Gaussian-type orbitals is still within the accuracy of Hartree-Fock solutions.[22]

In his development of the basis sets known as cc-pVXZ, Dunning uses the Gaussian-type orbitals shown by Huzinaga to be so effective. His basis sets incorporate higher angular momentum functions than those that are occupied by an atom to allow for correlation effects.[23] It had been shown previously that basis sets that are optimized for atomic correlation effects can be used to describe molecular correlation effects.[23] Dunning's basis sets are considered to be correlation consistent, meaning that each level of correlation adds about the same amount of energy.[23] This allows the basis sets to be built upon the lower level basis sets; in other words, cc-pVDZ correlation is used in cc-pVTZ and cc-pVTZ in cc-pVQZ. Focal point extrapolation

takes advantage of this building up principle to get the complete basis set limit for Hartree-Fock energies and correlation energies.

Another important aspect of computational chemistry is the variational method. It is this method that allows the guessing of a wavefunction for a description of a system.[24] The energy determined for any arbitrary guessed linear combination of test functions will always be higher than the true minimum energy of the system. This is very important for variational methods as there is now a limit for any computed energy.[24] It also allows close approximation of the true wavefunction since as the ansatz energy gets close to the true energy for a system, so to does the ansatz wavefunction get close to the true wavefunction of the system.[24]

In coupled cluster theory, the electronic wavefunction is expanded in terms of products of excited Hartree-Fock determinants. Coupled Cluster theory converges to an exact solution to the electronic Schrodinger equation for a given basis set, known as the full configuration limit (Full CI).[25] CCSD is the coupled cluster approximation using singles and doubles excited determinants for approximations. A benefit to this theory is that it is size consistent; coupled cluster theory becomes proportional to the number of particles(N) as $N \to \infty$.[25] The coupled cluster wavefunction can be written as $\psi = e^{\hat{T}}\phi_0$, where $\hat{T}$ is the cluster operator composed of excitation operators and ϕ_0 is the ground state Hartree-Fock wavefunction.[26] If the system is composed of A and B at infinite separation such that $\hat{T} = \hat{T}_A + \hat{T}_B$, the wavefunction goes to $\psi = e^{\hat{T}_A} e^{\hat{T}_B}\phi_0$. Since ϕ_0 can be split to describe A's and B's wavefunctions separately, the energy for this system is simply $E=E_A+E_B$.[26] This is known as size consistent. This differs from configuration interaction through easily seen math. The wavefunction for configuration interaction can be written as $\psi = (1+\hat{C})\phi_0$.[26] Using a similar setup as the coupled cluster A and

B scenario, $\hat{C} = \hat{C}_A + \hat{C}_B$. The wavefunction then becomes $\psi = (1 + \hat{C}_A + \hat{C}_B)\phi_0$.[26] Energy now no longer is a sum of the separated particles' energies, since the wavefunction is no longer multiplicatively separable. Thus, configuration interaction is not size consistent, while coupled cluster is size consistent.[26] One potential downside of this theory is that, since it is not actually a variational method, it is possible to obtain more than 100% of the correlation energy. Correlation energy is due to opposite-spin electron interactions and is the difference between the full CI energy and the Hartree-Fock limit.[25]

Density functional theory, as developed by Kohn and Sham, treats the electrons as a fluid with density. Because of the Born-Oppenheimer approximation, the nuclei of the atoms are considered fixed within this fluid of electrons.[27] The energy of the system is split into the non-interacting kinetic energy, the electrostatic energies due to both electron repulsion and nuclear attraction, and the exchange-correlation energy. The electrostatic energy is the simplest and needs no approximation.[27] The current approximations for the other terms cause many of the errors found in density functional theory. The Thomas-Fermi model used in approximations for the non-interacting kinetic energy works best for molecules of higher density.[27] Simple local density approximation yields incorrect analysis when van der Waals forces are involved since these are due to nonlocal correlations.[27]

The main failure of local density approximation is the assumption of a uniform electron density. Becke improved upon the exchange energy after realization that the spin-density gradients greatly improved density functional theory bond energies.[28] These gradients account for the non-homogeneous nature of electrons in a molecular system. Becke realized that a main reason bond energies in particular were incorrect using just local density approximation was that a bond was merely the overlap of two far limit tails.[28] Local density approximation fails in this

far limit. Becke's non-hybrid gradient corrected functional correctly reproduces the far limit and is exchange only.[28]

Becke showed in his second paper of three leading to the formulation of his hybrid functional known as B3 that his corrections to the exchange energy need to be accompanied by a good dynamic correlation approximation. If it is not, there is still considerable error due in part to self interaction energy.[29] He notes the need for gradient corrections for correctly approximating dynamic correlation. Though he uses a reparamaterized PW91, originally made by Perdew and Wang in 1991, in his second paper, LYP, by Lee, Yang, and Parr, works well too. Lee, Yang, and Parr based their work on Colle and Salvetti.[30] Colle and Salvetti argued that correlation can be approximated by the second order Hartree-Fock density matrix multiplied by a series of correlation factors. For their work, Colle and Salvetti parameterized for Helium.[30] Unfortunately, Helium is not a good model system for the rest of the elements. Lee, Yang, and Parr saw the potential of Colle and Salvetti's work by reworking their equations and reparameterizing with more than Helium as a benchmark. As part of their derivation, Lee, Yang, and Parr replaced the second order Hartree-Fock density matrix with the second order Kohn-Sham density matrix to make a pure, rather than hybrid, correlation only functional.[30]

In his third paper, Becke saw a need for a hybrid functional. He put a large emphasis on the adiabatic connection formula for the exchange and correlation components of Kohn-Sham density functional theory:[31]

$$E_{XC} = \int_0^1 U_{XC}^{\lambda} d\lambda \,.$$

This formula establishes a connection between the pure Kohn-Sham non-interacting system, $\lambda = 0$, and the fully interacting system, $\lambda = 1$, through a continuous series of mixed systems. The Pure Kohn-Sham non-interacting system energy is that of the Slater determinant exchange

energy and can be well approximated by the conventional Hartree-Fock eschange energy.[31] Once again, Becke compensates for a failure of local density approximation. Local density approximation causes an overbinding error because of a left-right correlation that is inappropriate when near this non-interacting limit.[31] Because of this, Becke introduces a Hartree-Fock term to his gradient corrected exchange only functional.

Density functional theory's advantage over other theories is its low computational cost and, when it works, accurate results. Density functional theory is benchmarked with focal point extrapolations in this work to show that it is accurate for this system.

Specific Theoretical Methods

Accurate relative energies and complexation energies of two isomers of $CN^{\cdot\cdot\cdot}H_2O$ and $CN^{-\cdot\cdot\cdot}H_2O$ were computed by systematic extrapolations of electronic energies within the focal point approach.[17-20] Geometries were first optimized using coupled cluster theory with single, double, and perturbative triple excitations [CCSD(T)] paired with the cc-pVTZ basis set.[23] This was accomplished using analytic gradients in the Mainz-Austin-Budapest (MAB) version of ACES II.[32] Within the focal point approach, one executes dual expansions of the one- and N-particle basis sets at this fixed optimized geometry. Extrapolations of a series of valence electronic energies enable the systematic approach to the complete basis set Born-Oppenheimer result. Details of the procedure have been described previously.[33] Corrections to the extrapolated valence electronic energies are appended to account for core-electron correlation, non-Born-Oppenheimer effects, zero point vibrational energies, and scalar relativistic effects.

Within the valence focal point analyses, the leading correlation contribution was computed using second-order Z-averaged perturbation theory, evaluated using MPQC 2.4.[34] We

have previously shown that ZAPT provides convergence characteristics similar to popular restricted open-shell Møller-Plesset theories but at a reduced computational cost.[35] Electron correlation was treated primarily using coupled cluster theory, including single, double (CCSD), perturbative or full triple [CCSD(T) and CCSDT] and perturbative quadruple [CCSDT(Q)] excitations. CCSDT(Q) is the quadruple excitation analog of the popular CCSD(T) approach, and has been shown to yield results that very nearly reproduce the full CCSDTQ method.[36] To avoid spurious predictions arising from spin-contaminated reference wavefunctions, restricted open-shell Hartree-Fock (ROHF) wavefunctions were used for all open-shell coupled cluster calculations[37] except CCSDT(Q). These methods are denoted ROHF-UCCSD, ROHF-UCCSD(T), and ROHF-UCCSDT. Since ROHF-reference CCSDT(Q) energies are not available, the (Q) correction was based on the difference between unrestricted CCSDT(Q) and CCSDT energies. Since spin-contamination is all but completely removed for perturbative quadruple excitation computations,[38] the use of unrestricted reference wavefunctions for the (Q) correction will have negligible effect on the final predicted energies.

Density functional methods were employed to study CN and CN^- with larger clusters of water. Specifically, the B3LYP functional[31] paired with a DZP++ basis set was used. The DZP++ basis set comprises Dunning's contraction of Huzinaga's double-ζ primitives,[22] augmented with an even-tempered set of diffuse functions on all atoms.[39,40] Geometries were optimized via analytic gradients, and harmonic vibrational frequencies were computed to confirm all reported structures were minima on the B3LYP/DZP++ potential energy surface. All B3LYP computations were done using QChem 3.1.[41] For the focal point analyses all CCSD, CCSD(T), and closed-shell MP2 energies were computed using Molpro 2006.1. The Mainz-

Austin-Budapest (MAB) version of ACES II was used for the CCSDT energies while MRCC[42], paired with MAB ACES II, was used for the CCSDT(Q) calculations.

CHAPTER 3

RESULTS AND DISCUSSION

Below we report a detailed study of the microsolvation of ·CN and CN^- in water. Benchmark geometries and relative energies are first provided for ·CN and CN^- with one water, followed by results for clusters with two and three waters.

$CN^{\cdots}H_2O$ and $CN^{-\cdots}H_2O$ Complexes

Using CCSD(T) paired with the cc-pVTZ basis set, two disparate isomers of $CN^{\cdots}H_2O$ (structures **I** and **II** in Fig. 1) were located. The higher-lying structure II features a traditional hydrogen bond with the CN nitrogen serving as the proton acceptor. The global minimum (**I**), on the other hand, does not involve hydrogen bonding but is instead bound by electrostatic interactions. Based on our focal point analyses, which are unfortunately only to the CCSD(T) level due to computational issues for a few structures, this structure lies 30.3 kcal mol^{-1} below the hydrogen-bonded structure **II**. There appears to be an error in the focal point for structure **II** that has yet to be determined since the CCSD(T) cc-pVTZ energy difference was 1.2 kcal mol^{-1} (4.3 kcal mol^{-1} in B3LYP/DZP++), the anomalous energy being that of structure **II**. For the cyanide anion, two low-lying structures were also located: the global minimum (**I**) features nitrogen as the proton acceptor while structure **II,** being 0.3 kcal mol^{-1} higher according to the focal point and 0.5 kcal mol^{-1} with B3LYP/DZP++, is held together by an interaction of the water hydrogen with the carbon atom of CN^-.

The geometry of CN(H_2O) structure **I** can be understood based on simple multipolar arguments. Ignoring contributions from the higher-order multipoles, one would predict a dipole-dipole complex of water and ·CN to adopt the C_{2v}-symmetric structure depicted in Fig. 3(a). This is precisely what Hartree-Fock theory predicts when paired with a DZ basis set, presumably because at this level of theory the dipole moment of ·CN is overestimated by about a factor of two. However, correlated *ab initio* methods predict the C_s symmetric geometry (Fig. 3c). This is due primarily to contributions from the interaction of the quadrupole of water with the dipole moment of CN radical. The latter conclusion is supported by the orientational dependence of the energy, demonstrated by the constrained optimized structures shown in Fig. 2. Motion about the O···CN angle is facile, with changes in this angle from the equilibrium value of 142º to 180º (Fig. 3b) accompanied by a mere 0.2 kcal mol^{-1} in energy. On the other hand, forcing this system to adopt a C_{2v}-symmetric structure (Fig. 3a) raises the energy by an additional 3.4 kcal mol^{-1}. This electrostatic interaction is energetically more favorable than the hydrogen bonding of water and the nitrogen of ·CN.

Figure 1: CN radical with one water.

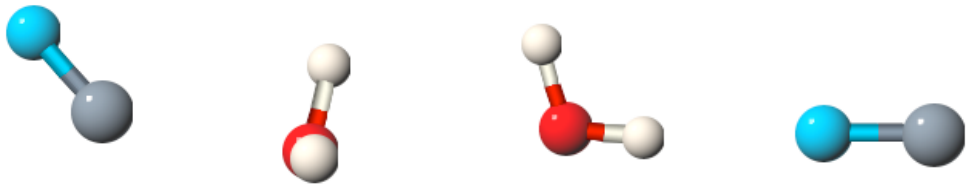

I **II**

Figure 2: CN anion with one water.

I **II**

Figure 3: Constrained structures of $NC^{\cdots}OH_2$ to explore the orientational dependence of the electrostatic interaction. Structure (a) was constrained to C_{2v} symmetry; in (b) the oxygen, carbon, and nitrogen are constrained to be co-linear; (c) is the unconstrained C_s-symmetric minimum (I). Relative energies are given in kcal mol-[1].

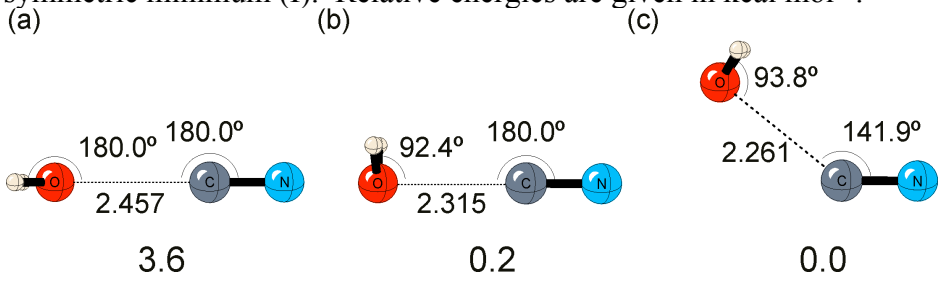

The stretching frequencies of both ·CN and CN^- increase when clustered with water. In both cases, the predicted shift in the CN stretching frequency is smaller for structure I than for II (see Tables 1 and 2). These predicted shifts in the ·CN stretching frequency should aid in the experimental identification of these complexes in molecular beams.

Table 1: Hydration energies ($E_{hydration}$, kcal mol^{-1}), vertical electron affinities (VEA, eV), and CN harmonic stretching frequencies [ω(CN str), cm^{-1}] of low-lying structures of $CN(H_2O)_n$.

N	$E_{hydration}$[a,b]		VEA	ω(CN str)[c]	
	FPA	B3LYP	B3LYP	CCSD(T)	B3LYP
0	-	-	4.03	2052.6	2121.7
1	1.6	5.6	2.71	2064.2	2130.3
2	-	9.8	2.36	-	2107.9
3	-	11.2	2.07	-	2117.0
4	-	9.3	1.95	-	2132.5

[a] FPA is the energy from a focal point analysis, as described above. B3LYP energies computed with the DZP++ basis set.
[b] $E_{hydration} = E[CN(H_2O)_n] - E[CN(H_2O)_{n-1}] - E(H_2O)$.
[c] ω(CN str) computed using CCSD(T) paired with the cc-pVTZ basis set.

To facilitate computations of larger clusters of ·CN and CN^- with water, we have benchmarked B3LYP/DZP++ against our focal point results for ·CN(H_2O) and CN^-(H_2O). For the complexes of ·CN and CN^- with one water, B3LYP/DZP++ predicted geometries are in reasonable agreement with the CCSD(T)/cc-pVTZ results discussed above. One notable exception is the B3LYP/DZP++ predicted geometry for structure I. Whereas CCSD(T)/cc-pVTZ predicts the C_s-symmetric structure to be a minimum, B3LYP/DZP++ predicts a similar C_s-symmetric structure to be a transition state (TS). This TS corresponds to the interconversion of two equivalent structures in which the CN radical is eclipsed with one or the other O-H bond of water. However, B3LYP predicts the TS to lie only 0.01 kcal/mol higher than the associated minima, consistent with the very small magnitude of the imaginary frequency computed at the TS (8i cm^{-1}). This energy difference is well below the zero point vibrational energy and, therefore, B3LYP/DZP++ effectively predicts a C_s-symmetric geometry consistent with the CCSD(T) results. It may also be noted that when paired with the 6-31G(d) basis set, B3LYP predicts a C_s-symmetric structure in accord with the coupled cluster result. One interesting thing to note is that the optimizations of CCSD(T) with cc-pVQZ that were tried, but abandoned due to length of computations, preferred C_1 symmetries for both one water CN radical structures.

The B3LYP results show fairly good agreement with the focal point analysis. The anion results were only apart by 1.7 kcal mol^{-1} (1.9 kcal mol^{-1} from experiment), and the radical results were only 4 kcal mol^{-1} apart. While the B3LYP predicted frequency shift for CN(H_2O) is in agreement with the coupled cluster results; for the CN^- anion, B3LYP overestimates the frequency shift by about 30 cm^{-1}.

Low-lying isomers of ·CN and CN^- with two, three, and four complexed water molecules were located at the B3LYP/DZP++ level of theory. Optimized structures are included in Figs. 4 and 5.

Table 2: Hydration energies ($E_{hydration}$, kcal mol^{-1}), vertical electron affinities (VEA, eV), and CN harmonic stretching frequencies [ω(CN str), cm^{-1}] of low-lying structures of $CN^-(H_2O)_n$.

n	$E_{hydration}$[a,b]			VDE		ω(CN str)[c]	
	Expt.	FPA	B3LYP	Expt.(T=12K)	B3LYP	CCSD(T)	B3LYP
0	-	-	-	3.862[43]	4.04	2068.6	2095.4
1	13.8[44]	14.0	15.7	4.54[43]	4.76	2082.4	2131.5
2	-	-	13.4	5.20[16]	5.35	-	2166.6
3	-	-	10.5	5.58[16]	5.58	-	2173.1
4	-	-	9.9	5.89[16]	5.89	-	2185.6

[a] FPA is the energy from a focal point analysis, as described above. B3LYP energies computed with the DZP++ basis set.
[b] $E_{hydration} = E[CN(H_2O)_n] - E[CN(H_2O)_{n-1}] - E(H_2O)$.
[c] ω(CN str) computed using CCSD(T) paired with the cc-pVTZ basis set.

$CN^{\cdots}(H_2O)_n$ and $CN^{-\cdots}(H_2O)_n$ Complexes

When CN and CN^- complex with more than one water, there becomes a noticeable difference in the structures of their minima. For $\cdot CN(H_2O)_n$, ring-like structures are preferred while $CN^-(H_2O)_n$ favors more linear chains. The ring structure for $\cdot CN(H_2O)_2$, $CN(H_2O)_3$, and$\cdot CN(H_2O)_4$ are favored despite a straining of bond angles from 141.6° on the carbon side of CN radical to 137.5° with two waters, 130.6° with three waters, and 130.5° with four waters. The nitrogen side has greater strain, going from 178.3° to 96.8° with two waters, 133.6° with three waters, 163.5° with four waters. These cyclic structures are made possible by the relative flatness of the potential energy surface along the $N\text{-}C^{\cdots}O$ bending angle in structure **I**.

The cyanide anion structures demonstrate that hydrogen bonding on the nitrogen side is preferable to hydrogen bonding on the carbon side. This is shown initially in the one-water structures, as the nitrogen hydrogen bonded structure is predicted to lay 0.5 kcal mol^{-1} below structure **II**. The two water structures indicate a preference for carbon-hydrogen connection over oxygen-hydrogen bonding of the first and second waters since the energetically minimum structure has a hydrogen bond on the carbon and the nitrogen, rather than having one water molecule bound to the nitrogen and the other water bound to the first water. The three water minimum further shows the preference of the nitrogen side with the third water complexing to the nitrogen side water of the dimer water structure.

As determined by B3LYP/DZP++, adding water to both CN radical and cyanide changes the stretching frequency of the CN relatively little after the first two waters are added. The most dramatic result is when CN has a second water added and forms a ring. This causes a significant drop in frequency of about 22.4 cm^{-1}. This data should provide a useful tool as the frequency increases only a little between the two and three water structures.

Electron affinities (EAs) of $\bullet CN(H_2O)_n$ can be readily computed using DFT.[39] Adiabatic EAs for $CN(H_2O)_n$ are included in Table 3 to study the evolution of the EA of CN upon hydration. The EA increases by almost 0.5 eV upon complexation with the first water, but then quickly levels off to a value of 4.6 eV. The decrease of vertical EAs with every water added as seen in Table 1 shows how unfavorable the oxygen-carbon interaction and ring complexes of the radical becomes upon addition of an electron.

The vertical detachment energies of Table 2 show very good agreement between the B3LYP/DZP++ results and that of experiment. They also show that, the anion structures are

unfavorable for the radical, though not nearly as unfavorable as the radical structures for the anion.

Table 3: B3LYP adiabatic electron affinities and CCSD(T) dipole moments.

System	Adiabatic EA(eV)	μ(Debye)
H_2O		1.9
CN^-		0.7
CN	4.04	1.3
$CN(H_2O)_1$	4.48	
$CN(H_2O)_2$	4.64	
$CN(H_2O)_3$	4.61	
$CN(H_2O)_4$	4.63	

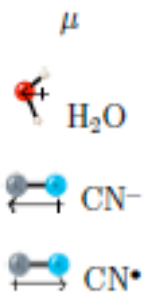

Figure 4: CN radical with two, three, and four waters.

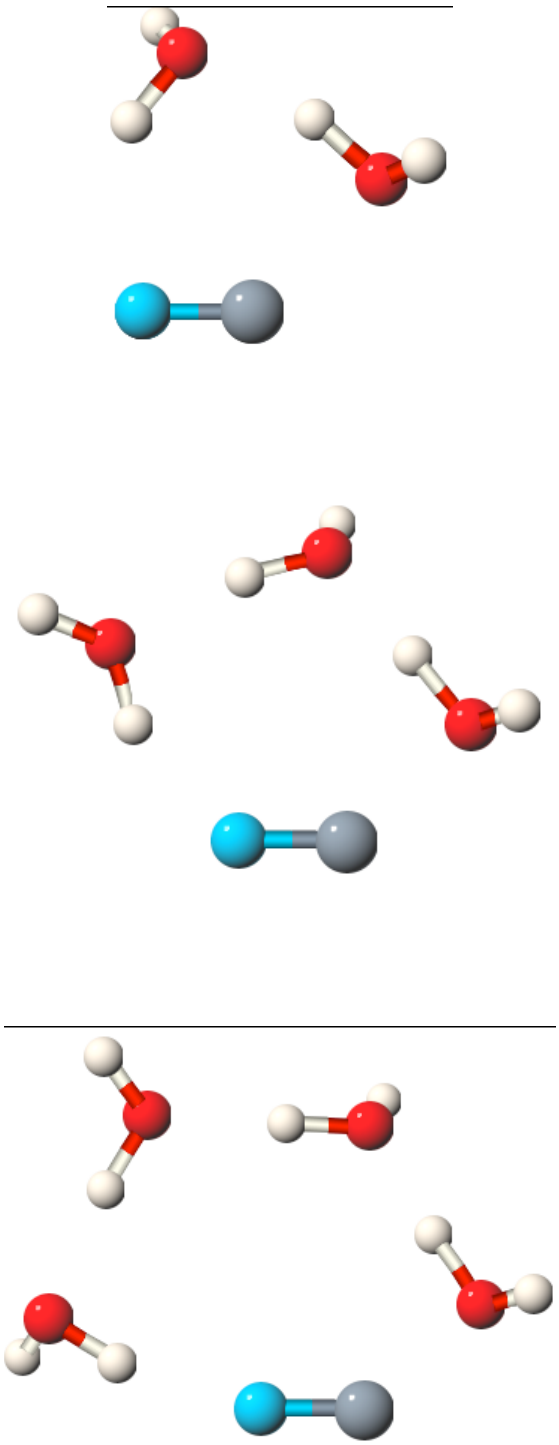

Figure 5: CN anion with two, three, and four waters.

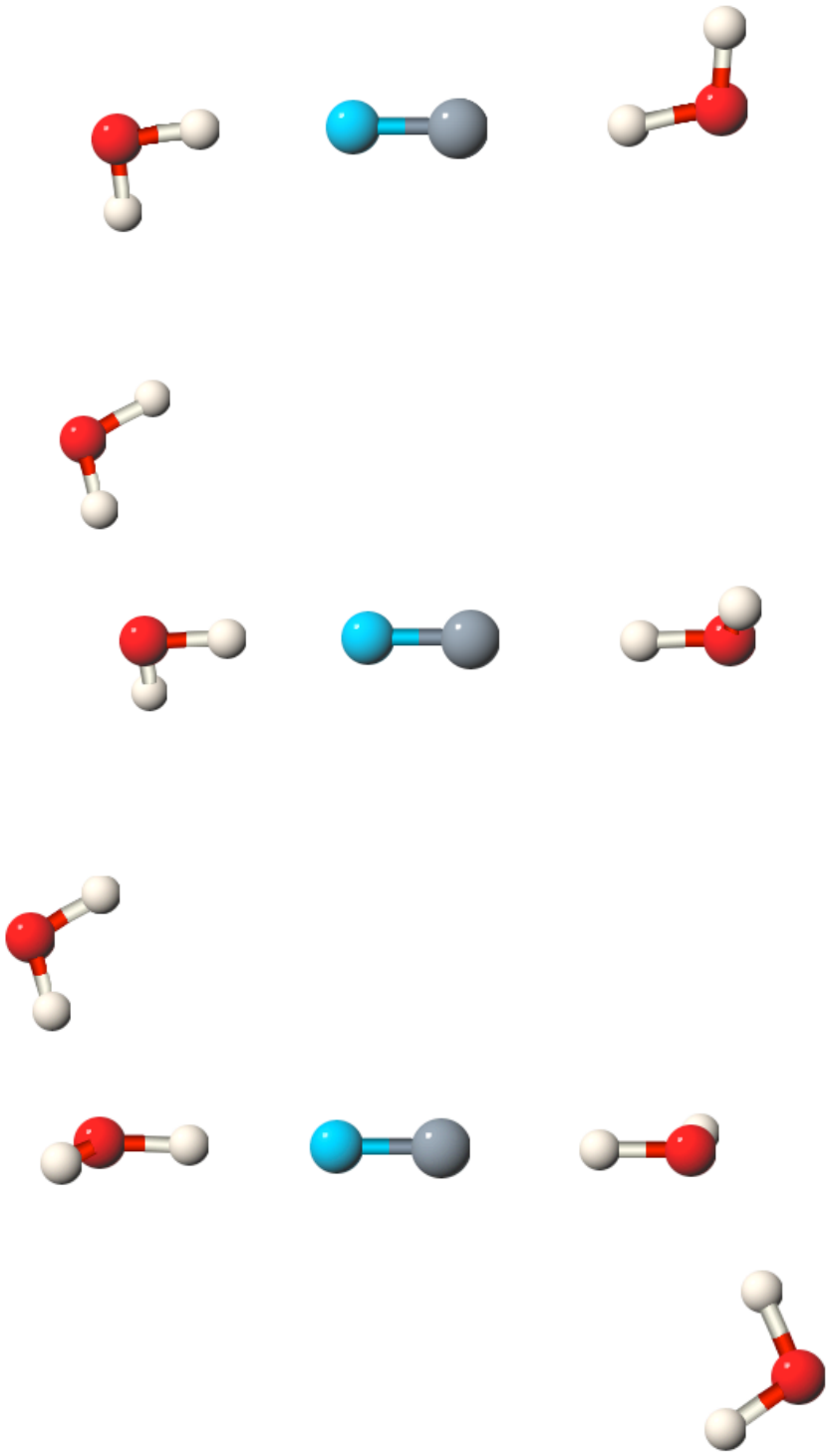

CHAPTER 4

SUMMARY AND CONCLUSIONS

We have shown that complexes of the CN radical with water form cyclic structures, while $CN^{-}\cdots H_2O$ adopts linear configurations. This prediction can be understood in terms of the more rigid nature of hydrogen bonding, compared to the dipole-quadrupole interactions. CN radical is capable of forming ring structures because these dipole-quadrupole interactions are relatively orientation independent and can accommodate larger deviations from optimal angles with little increase in energy. The stretching frequency of both the CN radical and cyanide anion increases, with one exception due to ring complexing, as they become hydrated. The change in frequency and electron affinity becomes smaller as water is added and the limit of many waters should be attainable in future work by studying larger $CN(H_2O)_n$ clusters.

Table 4: *Ab Initio* hydration energy focal point extrapolation for structure I of CN radical and one water, kcal mol^{-1}.

	HF	MP2/ZAPT2	CCSD	CCSD(T)
aug-cc-pVDZ	-1.25	-3.10	-2.51	-2.91
aug-cc-pVTZ	-0.92	-3.15	-2.55	-2.93
aug-cc-pVQZ	-0.86	-3.11	-2.50	-2.89
aug-cc-pV5Z	-0.83	[-3.09]	[-2.49]	[-2.87]
CBS LIMIT	[-0.83]	[-3.09]	[-2.48]	[-2.86]

Table 5: *Ab Initio* hydration energy focal point extrapolation for structure II of CN radical and one water, kcal mol^{-1}.

	HF	MP2/ZAPT2	CCSD	CCSD(T)
aug-cc-pVDZ	0.49	0.21	24.70	28.38
aug-cc-pVTZ	-0.16	-0.52	23.03	27.49
aug-cc-pVQZ	-0.09	-0.38	23.04	27.65
aug-cc-pV5Z	-0.08	[-0.35]	[+23.03]	[+27.69]
CBS LIMIT	[-0.08]	[-0.32]	[+23.01]	[+27.72]

Table 6: *Ab Initio* hydration energy focal point extrapolation for structure I of CN anion and one water, kcal mol^{-1}.

	HF	MP2/ZAPT2	CCSD	CCSD(T)
aug-cc-pVDZ	-12.63	-16.18	-15.45	-15.99
aug-cc-pVTZ	-12.56	-16.27	-15.55	-16.14
aug-cc-pVQZ	-12.38	-16.09	-15.32	-15.92
aug-cc-pV5Z	-12.35	[-16.06]	[-15.28]	[-15.88]
CBS LIMIT	[-12.35]	[-16.05]	[-15.25]	[-15.86]

Table 7: *Ab Initio* hydration energy focal point extrapolation for structure II of CN anion and one water, kcal mol^{-1}.

	HF	MP2/ZAPT2	CCSD	CCSD(T)
aug-cc-pVDZ	-11.45	-16.00	-14.94	-15.57
aug-cc-pVTZ	-11.35	-16.26	-15.19	-15.89
aug-cc-pVQZ	-11.20	-16.08	-14.96	-15.67
aug-cc-pV5Z	-11.18	[-16.05]	[-14.92]	[-15.64]
CBS LIMIT	[-11.18]	[-16.04]	[-14.89]	[-15.61]

Table 8: *Ab Initio* adiabatic electron affinity focal point extrapolation for the zero water case, eV.

	HF	MP2/ZAPT2	CCSD	CCSD(T)
aug-cc-pVDZ	3.394	3.873	3.693	3.678
aug-cc-pVTZ	3.394	4.021	3.834	3.817
aug-cc-pVQZ	3.389	4.068	3.875	3.857
aug-cc-pV5Z	3.389	[4.087]	[3.890]	[3.872]
CBS LIMIT	[3.389]	[4.106]	[3.907]	[3.889]

REFERENCES

(1) Wheeler, S. E. HFSmol; University of Georgia.

(2) Fray, N.; Benilan, Y.; Cottin, H.; Gazeau, M. C.; Crovisier, J. *Planetary and Space Science* **2005**, *53*, 1243.

(3) Chen, Y. R.; Deterding, L. J.; Tomer, K. B.; Mason, R. P. *Biochemistry* **2000**, *39*, 4415.

(4) Bumpus, J. A.; Tien, M.; Wright, D.; Aust, S. D. *Science* **1985**, *228*, 1434.

(5) Shah, M. M.; Grover, T. A.; Aust, S. D. *Archives of Biochemistry and Biophysics* **1991**, *290*, 173.

(6) Bockeleemorvan, D.; Crovisier, J.; Baudry, A.; Despois, D.; Perault, M.; Irvine, W. M.; Schloerb, F. P.; Swade, D. *Astronomy and Astrophysics* **1984**, *141*, 411.

(7) Bockeleemorvan, D.; Crovisier, J. *Astronomy and Astrophysics* **1985**, *151*, 90.

(8) Krasnopolsky, V. A. *Astronomy and Astrophysics* **1991**, *245*, 310.

(9) Ahearn, M. F.; Hoban, S.; Birch, P. V.; Bowers, C.; Martin, R.; Klinglesmith, D. A. *Nature* **1986**, *324*, 649.

(10) Bernstein, M. P.; Allamandola, L. J.; Sandford, S. A. *Advances in Space Research* **1997**, *19*, 991.

(11) Woon, D. E. *Icarus* **2001**, *149*, 277.

(12) Saal, A. E.; Hauri, E. H.; Cascio, M. L.; Van Orman, J. A.; Rutherford, M. C.; Cooper, R. F. *Nature* **2008**, *454*, 192.

(13) Solomonson, L. P. In *Cyanide in Biology*; Vennesland, B., European Molecular Biology Organization., Eds.; Academic Press: London ; New York, 1981; pp 11.

(14) Moreno, S. N. J.; Stolze, K.; Janzen, E. G.; Mason, R. P. *Archives of Biochemistry and Biophysics* **1988**, *265*, 267.

(15) Chen, Y. R.; Sturgeon, B. E.; Gunther, M. R.; Mason, R. P. *Journal of Biological Chemistry* **1999**, *274*, 24611.

(16) Wang, X. B.; Kowalski, K.; Wang, L. S.; Xantheas, S. S. *Journal of Chemical Physics* **2010**, *132*, 10.

(17) East, A. L. L.; Allen, W. D. *J. Chem. Phys.* **1993**, *99*, 4638.

(18) Allen, W. D.; East, A. L. L.; Császár, A. G. In *Structures and Conformations of Non-Rigid Molecules*; Kluwer: Dordrecht, 1993; pp 343.

(19) Császár, A. G.; Allen, W. D.; Schaefer, H. F. *J. Chem. Phys.* **1998**, *108*, 9751.

(20) Császár, A. G.; Tarczay, G.; Leininger, M. L.; Polyansky, O. L.; Allen, W. D. Dream or Reality: Complete Basis Set Full Configuration Interaction Potential Energy Hypersurfaces. In *Spectroscopy from Space*; Demaison, J., Sarka, K., Cohen, E. A., Eds.; Kluwer: Dordrecht, 2001; pp 317.

(21) Jackson, J. D. *Classical Electrodynamics*; John Wiley & Sons, Inc., 1975.

(22) Huzinaga, S. *Journal of Chemical Physics* **1965**, *42*, 1293.

(23) Dunning, T. H., Jr. *J. Chem. Phys.* **1989**, *90*, 1007.

(24) McQuarrie, D. A.; Simon, J. D. *Physical Chemistry: A Molecular Approach*; University Science Books, 1997.

(25) Szabo, A.; Ostlund, N. S. *Modern Quantum Chemistry: Introduction to Advanced Electronic Structure Theory*; Dover Publications, Inc., 1996.

(26) Crawford, T. D.; Schaefer, H. F. An introduction to coupled cluster theory for computational chemists. In *Reviews in Computational Chemistry, Vol 14*; Wiley-Vch, Inc: New York, 2000; Vol. 14; pp 33.

(27) Argaman, N.; Makov, G. *American Journal of Physics* **2000**, *68*, 69.

(28) Becke, A. D. *Journal of Chemical Physics* **1992**, *96*, 2155.

(29) Becke, A. D. *Journal of Chemical Physics* **1992**, *97*, 9173.

(30) Lee, C.; Yang, W.; Parr, R. G. *Physical Review B* **1988**, *37*, 785.

(31) Becke, A. D. *J. Chem. Phys.* **1993**, *98*, 5648.

(32) Stanton, J. F.; Gauss, J.; Watts, J. D.; Szalay, P. G.; Bartlett, R. J. w. c. f. A., A. A.; Bernholdt, D. E.; Christiansen, O.; Harding, M. E.; Heckert, M.; Heun, O.; Huber, C.; Jonsson, D.; Jusélius, J.; Lauderdale, W. J.; Metzroth, T.; Michauk, C.; O'Neill, D. P.; Price, D. R.; Ruud, K.; Schiffmann, F.; Varner, M. E.; Vázquez, J. a. t. i. p. M. A., J. and Taylor, P. R.), PROPS (Taylor, P. R.), and ABACUS (Helgaker, T.; Jensen, H. J. A.; Jørgensen, P.; and Olsen, J. F. t. c. v., see http://www.aces2.de.

(33) Schuurman, M. S.; Muir, S. R.; Allen, W. D.; Schaefer, H. F. *J. Chem. Phys.* **2004**, *120*, 11586.

(34) Janssen, C. L.; Nielson, I. B.; Leininger, M. L.; Seidl, E. T.; Colvin, M. E. MPQC 2.1.4; Sandia National Laboratories: Livermore, California, 2002.

(35) Wheeler, S. E.; Allen, W. D.; Schaefer, H. F. *J. Chem. Phys.* **2008**, *128*, 074107.

(36) Bomble, Y. J.; Stanton, J. F.; Kállay, M.; Gauss, J. *J. Chem. Phys.* **2005**, *123*, 054101.

(37) Roothaan, C. C. J. *Rev. Mod. Phys.* **1960**, *32*, 179.

(38) Stanton, J. F. *J. Chem. Phys.* **1994**, *101*, 371.

(39) Rienstra-Kiracofe, J. C.; Tschumper, G. S.; Schaefer, H. F.; Nandi, S.; Ellison, G. B. *Chem. Rev.* **2002**, *102*, 231.

(40) Lee, T. J.; Schaefer, H. F. *J. Chem. Phys.* **1985**, *83*, 1784.

(41) Shao, Y.; Fusti-Molnar, L.; Jung, Y.; Kussmann, J.; Ochsenfeld, C.; Brown, S. T.; Gilbert, A. T. B.; Slipchenko, L. V.; Levchenko, S. V.; O'Neill, D. P.; DiStasio Jr., R. A.; Lochan, R. C.; Wang, T.; Beran, G. J. O.; Besley, N. A.; Herbert, J. M.; Lin, C. Y.; Van Voorhis, T.; Chien, S. H.; Sodt, A.; Steele, R. P.; Rassolov, V. A.; Maslen, P. E.; Korambath, P. P.; Adamson, R. D.; Austin, B.; Baker, J.; Byrd, E. F. C.; Dachsel, H.; Doerksen, R. J.; Dreuw, A.; Dunietz, B. D.; Dutoi, A. D.; Furlani, T. R.; Gwaltney, S. R.; Heyden, A.; Hirata, S.; Hsu, C.-P.; Kedziora, G.; Khalliulin, R. Z.; Klunzinger, P.; Lee, A. M.; Lee, M. S.; Liang, W.; Lotan, I.; Nair, N.; Peters, B.; Proynov, E. I.; Pieniazek, P. A.; Rhee, Y. M.; Ritchie, J.; Rosta, E.; Sherrill, C. D.; Simmonett, A. C.; Subotnik, J. E.; Woodcock III, H. L.; Zhang, W.; Bell, A. T.; Chakraborty, A. K.; Chipman, D. M.; Keil, F. J.; Warshel, A.; Hehre, W. J.; Schaefer III, H. F.; Kong, J.; Krylov, A. I.; Gill, P. M. W.; Head-Gordon, M.; Gan, Z.; Zhao, Y.; Schultz, N. E.; Truhlar, D.; Epifanovsky, E.; Oana, M. Advances in methods and algorithms in a modern quantum chemistry program package; Qchem 3.1 ed.; *Phys. Chem. Chem. Phys.*, **2006**; *8*; 3172

(42) Kallay, M.; Surjan, P. R. *J. Chem. Phys.* **2001**, *115*, 2945.

(43) Wang, X. B.; Werhahn, J. C.; Wang, L. S.; Kowalski, K.; Laubereau, A.; Xantheas, S. S. *Journal of Physical Chemistry A* **2009**, *113*, 9579.

(44) Payzant, J. D.; Yamdagni, R.; Kebarle, P. *Canadian Journal of Chemistry* **1971**, *49*, 3308.